Carcinogenesis vol.18 no.5 pp.897–904, 1997

The role of UV-B light in skin carcinogenesis through the analysis of *p53* mutations in squamous cell carcinomas of hairless mice

Nicolas Dumaz[1,5,6], Henk J.van Kranen[2,6], Anja de Vries[2], Rob J.W.Berg[3], Piet W.Wester[4], Coen F.van Kreijl[2], Alain Sarasin[1], Leela Daya-Grosjean[1] and Frank R.de Gruijl[3]

[1]Laboratory of Molecular Genetics, Institut de Recherches sur le Cancer, B.P. no. 8, 94801 Villejuif, France, [2]Laboratories of Carcinogenesis and Mutagenesis, and [4]Pathology, National Institute of Public Health and Environmental Protection, PO Box 1, Bilthoven and [3]Institute of Dermatology, AZU, Utrecht University, The Netherlands

[5]To whom correspondence should be addressed

[6]These authors contributed equally to this work

Mutation spectra of the *p53* gene from human skin carcinomas have been connected to solar UV radiation. For comparison we have characterized the mutation spectrum of the *p53* gene in a very large sample of squamous cell carcinomas from hairless mice induced with UV of wavelength 280–320 nm (UV-B), which have substantiated the mutagenic effects of UV-B radiation *in vivo*. Tumors from hairless mice, random bred SKH:HR1 as well as inbred SKH:HRA strains, which are analyzed for mutations in the conserved domains of the p53 protein present a very specific mutation spectrum. The observed mutation frequency after chronic UV-B radiation in the *p53* gene ranged from 54% (SKH-HRA) to 73% (SKH-HR1) among the 160 tumors analyzed. Over 95% of the mutations were found at dipyrimidine sites located in the non-transcribed strand, the majority were C→T transitions and 5% were CC→TT tandem double mutations. Four distinct UV-B mutation hot spots have been identified for the first time: two major ones at codons 267 (33%) and 272 (19%) and two minor ones at codons 146 (10%) and 173 (4%). The codon 267 hot spot consists of a CpG preceded by a pyrimidine, which confirms *in vivo* an important role for this UV-B mutable site in UV-B-induced skin tumors that is not found in other types of mouse tumors. Comparison with mutation spectra from human skin carcinomas fully validates the merits of the hairless mouse model for studying the molecular mechanisms of skin carcinogenesis. For example, the murine hot spot at codon 272 does have a full equivalent in human skin carcinomas. In contrast, the human equivalent of the murine codon 267 lacks the dipyrimidine site and therefore fails to be a pronounced hot spot in human skin carcinomas; however, this site is one of the major hot spots in human internal cancers (evidently not induced by UV radiation but probably by deamination of the 5 methyl cytosine).

Introduction

The carcinogenicity of sunlight to the skin has been recognized for nearly a century and various experimental studies have clearly substantiated the causal role of UV light in non-melanoma skin cancers (1). However, the specific relationship between UV induced damage and skin cancer induction has only been substantiated in more recent years. Among the most compelling evidence, which demonstrate that DNA damage generated by solar UV is a critical component in the etiology of skin cancer, are the recent molecular epidemiological results obtained by studying the alterations of the *p53* gene in human skin cancers (2–4).

As in all other tissues, skin carcinogenesis is a complex process that involves many modifications including proto-oncogenes and tumor suppressor genes. Among these, the *p53* tumor suppressor gene has all the characteristics required for analyzing mutation spectra in tumors and enables elucidation of the events involved in the initiation of cancers (5). It is by far one of the most frequently mutated genes found in human cancers and can be functionally altered at more than a hundred different codons, which code for the amino acids clustered in the central hydrophobic region of the protein. Although all possible types of mutations have been documented, the majority consists of missense mutations. Moreover, the large database containing >4500 mutations of the *p53* gene in human cancers (6) has allowed the comparison of mutation spectra among different classes of human tumors.

It has already been shown that the *p53* mutation spectrum in human skin cancers is significantly different from those observed in other human cancers but very similar to those observed in UV-treated target genes in model systems (2,3). In human skin carcinomas, *p53* mutations are mainly C→T transitions located on dipyrimidine sites that are specific UV targets, whereas in internal cancers C→T are mainly located at CpG sites. Moreover CC→TT tandem substitutions, generally recognized as being the characteristic fingerprint of UV lesions, are frequently found in human skin carcinomas (7–11).

Skin carcinogenesis experiments with animal models, particularly the mouse, have already yielded a lot of data on how skin tumor development depends on dose, time and wavelength of the UV-radiation (12). Indeed, murine skin cancers induced by repeated exposure to UV radiation provide an excellent model system for investigating the molecular mechanisms of UV carcinogenesis, since UV radiation is the only carcinogenic agent known once other known risk factors are carefully controlled for or eliminated. In particular, studies on hairless mice have demonstrated that wavelengths in the UV-B (280–320 nm) region of the solar spectrum are the most carcinogenic (13).

Therefore, in the present study we were particularly interested in looking for *p53* alterations in UV-B-induced murine skin cancers in order to investigate whether the relationship between oncogenetic changes and the UV radiation described for human non-melanoma skin cancers could be confirmed in the hairless murine model. Up to now, the data from various studies have been conducted on relatively small sample sizes that have ranged from 11 to 30 tumors induced by UV-B in a

***Abbreviations**: SCC, squamous cell carcinomas; SSCP, single strand conformation polymorphism; UV-B, UV with a wavelength of 280–320 nm; XP, xeroderma pigmentosum.

variety of mice including normal and hairless strains (14–16). The present study aimed to produce a detailed mutation spectrum of the *p53* gene in the mouse model to enable a better comparison with human data. To this end we have carried out a project in which two large series of skin tumor samples (~160 tumors in total) were analyzed separately in two collaborating laboratories. The results from the two experimental groups have confirmed the strong evidence for the involvement of UV-induced damage in *p53* modifications in squamous cell carcinomas (SCC*). Moreover, the p53 protein is a highly conserved molecule that allows data from animal models to be extrapolated to man. Hence, for the first time, the present study has allowed us to compare the very specific *p53* mutation spectra obtained from our large study in UV-B-induced murine skin cancers with those observed in solar induced human skin cancers, and has thus confirmed and substantiated in more detail the role of UV-B in solar mutagenesis and skin carcinogenesis in man.

Materials and methods

Tumor induction and DNA isolation: Groups I and II

The experimental procedure used for tumor induction by chronic UV-B radiation in albino hairless mice has been previously described in detail (17). In brief, SKH-HRA (inbred strain, 18 mice) or SKH-HR1 (random bred, 40 mice) mice were irradiated daily for 75 min intervals with UV-B, starting at 10 weeks of age. The daily surface exposure on the dorsal area of the mice was 150 mJ/cm^2 of UV emitted from Westinghouse FS40 sun-lamps (with a maximum output wavelength around 310 nm). After 10 weeks the first tumors appeared and after 25 weeks all mice had multiple dorsal skin tumors. Group I mice were killed at 25 weeks and six Group II mice were killed at week 18 and 12 Group II mice at week 25. After killing, the tumors were carefully removed. Tumors collected from the SKH-HR1 mice were designated Group I and analyzed in Villejuif, whereas tumors from the SKH-HRA strain were designated Group II and analyzed in Bilthoven. To prepare tumor tissue for histology and immunohistochemical analysis of p53, only a portion of the tumors from Group II was formalin fixed for ± 18 h and paraffin embedded according to routine procedures. The other portion, or for Group I the whole tumor, was snap-frozen in liquid N_2 and stored at –80°C for molecular analysis. Isolation of DNA for mutation analysis was performed as described previously for Group I (18) and by other standard methods (19) for Group II.

Group I

Single-strand conformation polymorphism (SSCP) analysis

The coding region of the *p53* gene corresponding to the central region of the protein was amplified by using six sets of primers covering exons 5, 6, 7 and 8. To avoid amplification of the mouse *p53* pseudogene, all primers were located in the introns or spanned the intron–exon junctions. The following primer couples were used: ME5F-ME5R for exon 5, ME5F-ME5–6R for exons 5 and 6, ME7F-ME7R1 and ME7F-ME7R2 for exons 7, ME8F1-ME8R1 and ME8F2-ME8R2 for exon 8. The sizes of the amplified fragments were respectively 204 pb, 425 bp, 257 bp, 231 bp, 269 bp and 157 bp. The sequences of the primers were as follows:

ME5F 5′-TCTCTTCCAGTACTCTCCTC-3′
ME5R 5′-GAGGGCTTACCATCACCATC-3′
ME5–6R 5′-AATTACAGACCTCGGGTGGCT-3′
ME7F 5′-GCCGGCTCTGAGTATACCACCAT-3′
ME7R1 5′-GGAAACAGAGGAGGAGACTTCAT-3′
ME7R2 5′-GGTAGATAGGGTAGGAAC-3′
ME8F1 5′-TCTTACTGCCTTGTGCTGGTCCT-3′
ME8F2 5′-TCCCGGATAGTGGGAACCTT-3′
ME8R1 5′-CAGGTGGGCAGCGCTGTGGAAGG-3′
ME8R2 5′-GCCTGCGTACCTCTCTTTGC-3′

Genomic DNA (100–500 ng) was incubated in a total volume of 25 µl containing dNTP at 100 µM each, 0.2 µM of each primer and 1 U of GoldStar DNA polymerase (Eurogentec, Belgium), 5 µCi of [α^{32}P]dCTP (Du Pont/NEN, USA) buffered in 75 mM Tris–HCl pH 9.0, 20 mM $(NH4)_2SO_4$, 0.01% (w/v) Tween 20, 1.5 mM $MgCl_2$. For the analysis of exon 8 a modification was applied using [α^{33}P]dCTP to enhance resolution of shifted bands especially for codon 267. The reaction mixture was heated at 92°C for 2 min and amplification was carried out for 30 cycles of 92°C for 1 min, 50°C or 55°C for 1 min and 72°C for 2 min. The reaction was stopped after 5 min at 72°C by a 10-fold dilution into 0.01% SDS, 10 mM EDTA. Aliquots of 4 µl of this solution were then mixed with 7 µl of 95% (v/v) formamide, 20 mM EDTA, 0.05% bromophenol blue and 0.05% xylene cyanol. The samples were denatured for 5 min at 100°C, quick-chilled on ice for 3 min and loaded immediately onto a 0.5% MDE (Bioprobe Systems) gel containing 0.6× TBE (1× TBE contains 89 mM Tris, 80 mM boric acid and 2 mM EDTA) with or without 10% glycerol. Electrophoresis was carried out at constant power (4, 6, 8 or 10 W) for 16 to 22 h at room temperature or at 8°C in a cold room (for gels without glycerol). After migration, gels were dried and subjected to autoradiography. The entire procedure was repeated at least twice for each sample. When shifted bands were observed, they were cut out of the gel, the DNA was eluted in distilled water and reamplified as described.

Purification and sequencing of the PCR products

The PCR products were purified on an agarose gel and the DNA extracted using the Nucleotrap kit (Macherey Nagel, Germany). Purified products were directly sequenced using the Sequenase version 2.0 kit (USB/Amersham) or cloned into a pUC 18 vector by the Sure Clone Ligation Kit (Pharmacia, Sweden) before being sequenced.

Group II

Immunohistochemistry

Immunohistochemical staining was carried out on deparaffinized 5-µm sections, using the CM-5 polyclonal antibody (kindly provided by Dr David Lane) and counterstained with hematoxylin as previously described (16). For histological diagnostic purposes, serial sections of all samples were also stained with hematoxylin and eosin (H&E).

DNA amplification

Exons 4 to 8 of the *p53* gene were individually amplified from DNA isolated from tumors and control tissue as described previously (16). The following pairs of primers, in which ‘e’ and ‘i’ stand for exon and intron respectively, were used. Sense (s) represents the 5′ oligo whereas antisense (as) represents the 3′ oligo

Exon 4: e4m2s: 5′-CCCCTGTCATCTTTTGTCCC-3′
i4las: 5′-TCAGGGCAAAACTAAACTCT-3′
Exon 5: i4rs: 5′-AGTTCCCCACCTTGACACCT-3′
i5ras: 5′-AGAGCAAGAATAAGTCAGAA-3′
Exon 6: i5rs: 5′-ACTGGCAGCCTCCCATCTTCCC-3′
i6las: 5′-GTCAACTGTCTCTAAGACGCA-3′
Exon 7: i6rs: 5′-TGTAGTGAGGTAGGGAGCGAC-3′
i7las: 5′-CTGGGGAAGAAACAGGCTAA-3′
Exon 8: i7rs: 5′-CTTGTGCTGGTCCTTTTCTTG-3′
i8las2: 5′-AGGAGAGAGCAAGAGGTGACT-3′

The PCR conditions were as follows. Genomic DNA (100–200 ng) was incubated in a total volume of 100 µl with 0.5 µM of each primer, 250 µM of dNTPs, PCR buffer (50 mM KCl, 10 mM Tris–HCl pH 8.3, 3 mM $MgCl_2.6H_2O$, 0.001% gelatine) and 2.5 U of Taq polymerase (Perkin–Elmer). After an initial denaturation of 5 min at 95°C, amplification was performed for 30 cycles consisting of 30 s at 95°C, 1 min at 55°C and 2 min at 72°C using a Perkin–Elmer Thermal Cycler 9600. The concentration and length of the amplified fragments was checked by electrophoresis on a 3% agarose gel (FMC Bioproducts, USA). Direct sequencing of the PCR products was performed as described previously (16).

Results

Tumor induction

Groups I and II. Induction of skin tumors in the hairless SKH mice by repeated UV-B radiation was as described in the Materials and methods. The use of different SKH strains in this study was essentially for practical reasons as only the randomly bred HR1 strain is commercially available enabling the large sample size analyzed by Group I to be possible, and the inbred HRA strain, which has a lower breeding efficiency, accounts for the limited number of animals that could be studied in Group II. No differences were seen in UV-B tumor induction between the groups, and their mutiplicity ranged between 3–9 lesions per mouse independent of the strain. In Group I (SKH-HR1), all the lesions, which were SCC, were collected at week ~25. In Group II (SKH-HRA), 14 lesions were already collected at week 18, the remaining lesions were

collected at week ~25. A non-selective subset of these lesions were characterized histologically (H&E staining). The early lesions corresponded to actinic keratosis (AK) in man, which are considered to represent pre-malignant precursors of SCC. These early pre-cancerous lesions were frequently of the hypertrophic (papillomatous) form. Due to the histopathological heterogeneity within such a lesion and the often limited size of tumor sample, not all aspects of actinic keratosis (such as dysplasia) could be equally well demonstrated. Nevertheless these lesions were tentatively diagnosed as actinic keratosis. In a number of cases the skin lesions showed severe dysplasia and frank (local) invasion, leading to the diagnosis of SCC. All *p53* mutation analysis carried out in Group II was on SCC.

Frequency of p53 mutations

Once the tumors from the two groups were analyzed, the two different methods applied by both laboratories were compared to each other by exchanging some 20 isolated tumor DNAs. The outcome of this comparison confirmed the prevalence and types of mutations detected (Table I). However, at present, it is not clear yet whether the observed statistically significant difference between the frequencies for the SKH-HRA (53%) and the SKH-HR1 (73%) mice was really strain-specific or caused by a higher sensitivity of the SSCP method in detecting low abundance mutated alleles in a heterogeneous sample. It is, however, important to note that SSCP analysis for codon 267 in exon 8 needed an adaptation (see Materials and methods section) to prevent an underestimation of mutations at this position. This may be the reason why this important hot spot has not been recognized in earlier studies of UV-B induced *p53* mutation in the mouse (14,15).

Group I (SKH-HR1). The combined used of PCR and SSCP has provided a simple and sensitive method for the detection of point mutations. It has been observed that, depending on running conditions and primers used for PCR amplification, efficiency of the SSCP analysis may vary with the sequence context targeted for the screening of mutations (20,21). Recent results on different loci have proved that the combined use of different running conditions can enhance the detection sensitivity of this technique by up to 80–100% (22,23). Therefore to avoid underestimating the number of mutations in the *p53* gene detected by the SSCP analysis, several sets of primers and different gel running conditions were used in our study for each exon analyzed. SSCP analysis of exons 5 to 8 of the *p53* gene was carried out on 117 SCC as well as on four control normal skin biopsies. A total of 73% (85/117) of the tumors analyzed presented at least one base substitution on the *p53* gene whereas normal skin biopsies contained only wild-type sequences. All the mutations are listed in Table I. Among all mutated samples, 22 carried two distinct mutations and three tumors carried three distinct mutations. The fact that ~20% of the tumors contained multiple mutant alleles suggests that either the tumors were made up of heterogeneous population of cells or that mutant alleles with single base changes were targets of secondary mutation events, because of continued exposure to UV radiation during tumor progression. Furthermore wild-type sequences were always present together with mutated sequences in tumors, and the ratio of mutated to wild-type sequence varied considerably between the samples analyzed. The detection of signals for the wild-type allele was due either to the presence of normal tissue in the tumor biopsies or because only one allele had mutated.

Group II (SKH-HRA). Direct sequencing of exons 4 to 8 of the *p53* gene was carried out on 43 SCC isolated from 18 mice as well as on five normal skin biopsies. In 57% (8/14) of the tumors isolated after 18 weeks and in 52% (15/29) of the tumors isolated after 25 weeks, at least one base substitution in the *p53* gene was observed. Because the difference between these two subgroups is not statistically significant, we pooled the two and calculated that the average frequency to be 53%. Among the mutated samples, five carried two independent mutations, which is in agreement with the findings in Group I. All mutations for this group are listed in Table I. The presence of wild-type *p53* sequences noted for Group I also pertains to Group II.

Immunohistochemistry

Group II (SKH-HRA). A total of 83% (29/35) of the samples showed positive immunostaining with the CM-5 polyclonal antibody, which comprised 10–80% of the cells in the lesion. The type of nuclear immunostaining was basically the same as described previously (16). A typical example of tumors collected at week 18 and week 25 from Group II is presented in Figure 1. The positive predictive value of IHC for mutations in the conserved domains was 46%, whereas in 34% of the samples overexpression of *p53* was observed in the absence of any detectable mutations in the domains investigated. In ~10% of the cases, mutations were found without accompanying positive IHC. Finally, *p53* immunostaining was clearly visible in precursor lesions of AK already collected after 10 weeks of UV-B irradiation, although the staining was mainly confined to the basal layer (data not shown).

Characteristics of the p53 mutation spectrum

Groups I and II. All the mutations observed were missense mutations, except for one nonsense mutation and two silent mutations located on the third base of the codon, which were both associated with a second mutation in the sample. As shown in Tables I and II, most mutations (>80%) are C to T transitions, which are mainly located at CC and TC sites, with only a few (4/114) located at non-dimer CpG sites. However, when a CpG site like the one at codon 267, was preceded by a pyrimidine, thereby providing a putative cyclobutane dimer site, a high mutation frequency was observed. Tandem substitutions were frequent (10%) and consisted mainly of the characteristic CC→TT tandem transition. All but two tandem substitutions resulted in a single amino acid change. Nearly all mutations were targeted at dipyrimidine sites known to be UV photolesion hot spots [cyclobutane pyrimidine dimers or pyrimidine(6–4)pyrimidone photoproducts]. Association of the mutations with a dipyrimidine target site on the transcribed or the non-transcribed strand of the *p53* gene, demonstrated a strong strand bias towards the non-transcribed strand of the *p53* gene. Figure 2 shows the distribution of mutations along the *p53* gene. They were mainly (96%) located at evolutionary conserved regions of the gene and many have contributed to the four hot spots of mutations observed (amino acids 146, 173, 267 and 272).

Comparison of the murine and the human p53 mutation spectra

In order to ascertain the functional relevance of the *p53* mutation spectrum that was found in UV-B-induced murine skin cancer, we compared it to the *p53* mutation spectra found in normal human skin cancers or in skin cancers from xeroderma pigmentosum (XP) patients. XP is a rare inherited

Table I. Summary of all *p53* mutations detected in SCC from SKH-HR1 (Group I) and SKH-HRA (Group II) mice

Codon[a]	Sequence[b]	Strand[c]	Amino acid	Number of mutations		
				SKH-HR1	SKH-HRA[d]	Total
123–124	ccC Ctc→ccT Ttc	NT	Pro-Leu→Pro-Phe		1	1
124	ccc Ctc→ccc Ttc	NT	Leu→Phe		1	1
125	aaT aag→aaA aag	n.d.	Asn→Lys		(1)	(1)
137	gTg→gCg	n.d.	Val→Ala	1		1
	gTg→gGg	n.d.	Val→Gly		2	2
138	gtg Cag→gtg Tag	n.d.	Gln→Stop	1		1
145	aca Cct→aca Tct	NT	Pro→Ser	1		1
146	cct Cca→cct Tca	NT	Pro→Ser	11		11
	cCa→cTa	NT	Pro→Leu	2	2	4
148	gGg→gAg	T	Gly→Glu	1		1
149	ggg Agc→ggg Ggc	T	Ser→Gly	1		1
151–152	gtC Cgc→gtT Tgc	NT	Val-Arg→Val-Cys	1		1
153	gCc→gTc	NT	Ala→Val	1		1
155	gcC atc→gcT atc	NT	Ala→Ala	1		1
157	atc Tac→atc Aac	NT	Tyr→Asn	3		3
164–165	acG Gag→acA Aag	T	Thr-Glu→Thr-Lys	1		1
171	tgc Ccc→tgc Tcc	NT	Pro→Ser	1		1
	tgc cCc→tgc cTc	NT	Pro→Leu	1	1	2
172–173	caC Cat→caA Tat	NT	His-His→Gln-Tyr	1		1
173	cac Cat→cac Tat	NT	His→Tyr	3	2	5
184	cCt→cTt	NT	Pro→Leu	1		1
185	cct Ccc→cct Tcc	NT	Pro→Ser	1		1
188–189	ctT Atc→ctC Ttc	NT	Leu-Ile→Leu-Phe	1		1
235	tCc→tTc	NT	Ser→Phe	3		3
235–236	tcC Tgc→tcT Agc	NT	Ser-Cys→Ser-Ser	1		1
237–238	atG Ggg→atT Tgg	T	Met-Gly→Ile-Trp	1		1
239	GGc→AAc	T	Gly→Asn	1		1
242	aac Cgc→aac Tgc	NT	Arg→Cys	1	1	2
244	cCT→cTA	NT	Pro→Leu	1		1
246	cTt→cCt	NT	Leu→Pro	1	3	4
247	aCc→aTc	NT	Thr→Ile	1		1
257–258	aaC Ctt→aaT Ttt	NT	Asn-Leu→Asn-Phe	1		1
258	aac Ctt→aac Ttt	NT	Leu→Phe	(1)		(1)
259	cTg→cGg	NT	Leu→Arg	1		1
260	gGa→gAa	T	Gly→Glu	1		1
261	cGG→cAT	T	Arg→His	1		1
263–264	agC Ttt→agT Att	NT	Ser-Phe→Ser-Ile	1		1
264	tTt→tCt	NT	Phe→Ser	1		1
	agc Ttt→agc Ctt	NT	Phe→Leu		1	1
265	ttt Gag→ttt Aag	T	Glu-Lys	1		1
266	gag Gtt→gag Att	T	Val→Ile	1		1
267	gtt Cgt→gtt Tgt	NT	Arg→Cys	34	12 (16)	46 (50)
	gtt Cgt→gtt Agt	NT	Arg→Ser		1	1
268	gTt→gGt	NT	Val→Gly	1		1
271	tGc→tTc	n.d.	Cys→Phe	1		1
271–272	tgC Cct→tgT Tct	NT	Cys-Pro→Cys-Ser	2		2
272	tgc Cct→tgc Tct	NT	Pro→Ser	9	1 (2)	10 (11)
	tgc Cct→tgc Act	NT	Pro→Thr		(1)	(1)
	tgc CCt→tgc TTt	NT	Pro→Phe	1		1
	cCt→cTt	NT	Pro→Leu	10	1 (2)	11 (12)
	cCt→cAt	NT	Pro→His	2		2
	cCt→cGt	NT	Pro→Arg	1		1
283	ttC cgc→ttT cgc	NT	Phe→Phe	1		1
288–289	gtC Ctt→gtT Gtt	NT	Val-Leu→Val-Val	1		1
294	cCc→cTc	NT	Pro→Leu	2		2
	ccC→ccT	NT	Pro→Pro	1		1
Total (tandem taken as 1 mutation)				114	33 (42)	147 (156)
Total (tandem taken as 2 mutations)				126	37 (46)	163 (172)
Total number of mutated tumors (%)				85 (73%)	23 (53%)	108 (68%)

[a]Codon numbers are according to Soussi *et al.* (24).
[b]Sequence of the non-transcribed strand (5′→3′) is shown and the mutated bases are indicated in capital letters.
[c]The location of the bipyrimidine sequence where the mutation takes place on the transcribed (T) and the non-transcribed (NT) strand is indicated. n.d., indicates the absence of a possible dipyrimidine sequence at the mutated site.
[d]The numbers in parentheses include the mutations already found by van Kranen *et al.* (16) in UV-B-induced SKH-HRA skin tumors.

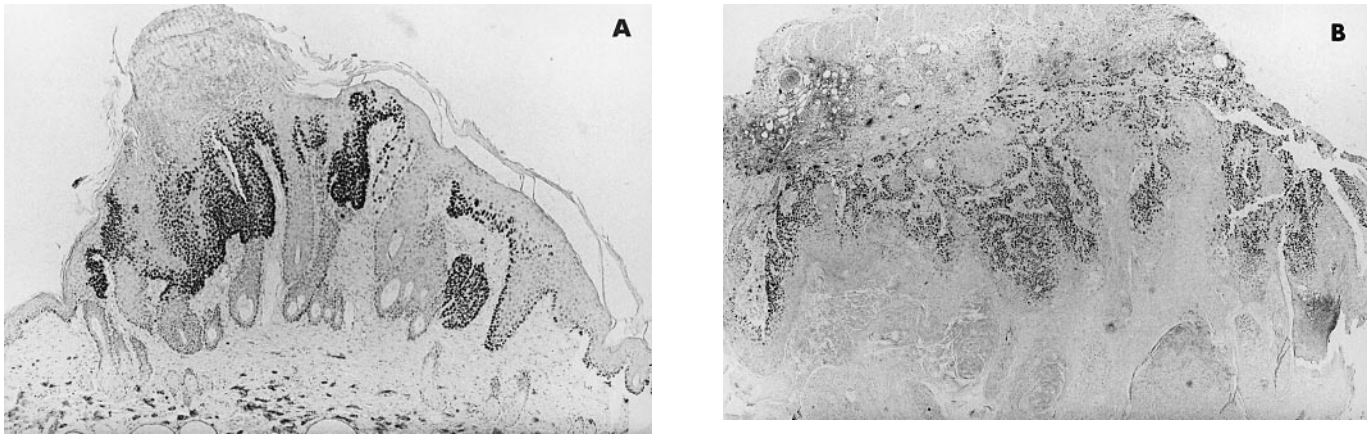

Fig. 1. Positive immunohistochemical staining of the p53 protein in tumor samples collected respectively at 18 (**A**) and 25 (**B**) weeks from Group II (SKH-HRA) mice.

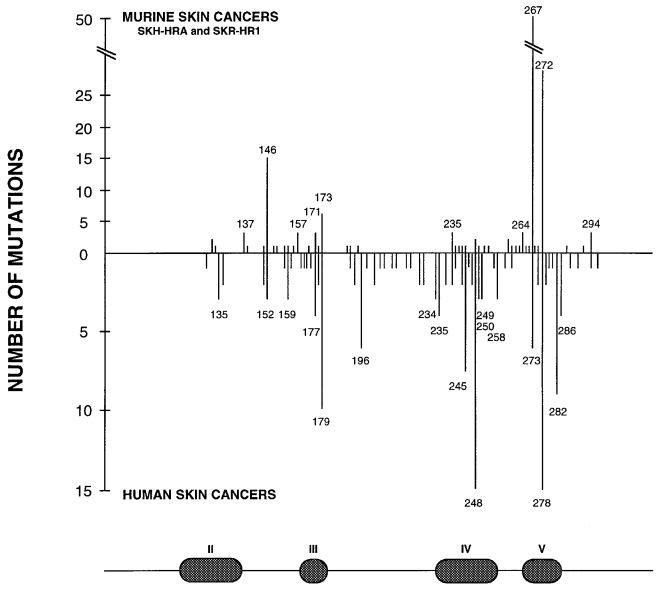

Fig. 2. Distribution of mutations along the *p53* gene. The localization of the mutations from murine cutaneous SCC (SKH-HR1 and SKH-HRA) at the top, is compared to those from human skin tumors (non-XP and XP patients) at the bottom. The position of the hot spots are indicated. Four of the highly conserved domains of the p53 protein are represented above the graph according to Soussi *et al.* (24). There is a codon numbering discrepancy between the human and mouse coding sequences, so codon 272 (mouse) corresponds to codon 278 (human) etc.

disease characterized by a deficiency in DNA repair associated with an extremely high level of skin tumors on exposed sites of the body. In a previous study we characterized the *p53* mutation spectrum in a series of cutaneous carcinomas from patients with XP (10). The mutations were almost all located at dipyrimidine sites. They were characterized by a high level of C→T and especially CC→TT transitions with the py–py sequences exclusively located on the non-transcribed DNA strand of these excision-repair deficient patients (10). Table II shows that the substitution type and their location at dipyrimidine sites are similar in murine and normal human skin cancers [data taken from several studies, see Reference (2) for review] and even more so in murine and XP skin tumors. The frequency of tandem substitutions was nearly the same in murine and non-XP human skin cancers whereas this frequency was significantly higher in XP tumors. The only significant difference between murine and human skin cancers was the strand location of dipyrimidine photolesions, which resulted in the *p53* mutations. As in the skin tumors of individuals with highly deficient DNA repair (XP complementation groups A and C), *p53* mutations in the UV-B-induced murine skin tumors arose mainly from unrepaired UV lesions on the non-transcribed strand of the gene, whereas in skin tumors from normal individuals, *p53* alterations did not show this strand bias. Figure 2 allows us to compare the distribution of *p53* mutations along the gene between murine and human skin carcinomas. The spectra are not exactly identical even though there are some common hot spots.

Discussion

The specificity of p53 mutations in UV-B-induced murine skin cancers

The analysis of mutation spectra has proven to be a powerful tool in identifying (solar) UV light as the major carcinogen for skin cancers by virtue of the unique and characteristic pattern of mutations created by it. It is obvious from the data presented here that the *p53* mutation spectrum observed in UV-B-induced murine skin cancers is UV-specific and very similar to those observed in other UV-B-treated target genes in model systems (25,26). These characteristics include the location of nearly all mutations (96%) on dipyrimidine sequences known to be targets for UV-induced photolesions, such as cyclobutane pyrimidine dimers and pyrimidine(6–4)pyrimidone photoproducts, while py–py sites are distributed randomly over the *p53* gene. Moreover, most mutations (81%) are GC to AT transitions whose presence could be explained by the hypothetical 'A rule' whereby the DNA polymerase is thought to incorporate preferentially an adenine opposite a non-instructive dipyrimidine photolesion. More significantly, a high level (10%) of tandem mutations, especially CC→TT double transitions, are found in the *p53* gene in murine skin cancers. These tandem substitutions are very characteristic of UV-induced mutagenesis and are considered an essential part of the fingerprint in UV photolesions, although it should be realized that oxidative damage can also result in CC→TT double transitions, although at a very low frequency (27). Interestingly, in eight of the 15 sites where tandem mutations were detected, the first mutation occurred on the third base of the 5′ codon and hence there was no change in the first amino acid involved in the mutation site. This clearly indicates that there was no selection pressure for this mutation and therefore

Table II. Distribution of single and tandem mutations on the *p53* gene in SKH-HR1 (Group I) and SKH-HRA (Group II) murine SCC and in non-melanoma human skin tumors

	In UV-B induced murine skin tumors			In human skin tumors	
p53 Mutations	SKH-HR1 (%)	SKH-HRA[a] (%)	Total[a] (%)	Non-XP (%)	XP (%)
Substitution type (single + tandem mutation/tandem taken as two mutations)					
GC→AT	106 (84)	34 (74)	140 (81)	57 (68)	39 (87)
GC→TA	4 (3)	5 (11)	9 (5)	12 (14)	2 (4)
GC→CG	2 (2)	0 (0)	2 (1)	9 (11)	0 (0)
AT→GC	5 (4)	4 (9)	9 (5)	3 (4)	1 (2)
AT→CG	2 (2)	2 (4)	4 (2)	0 (0)	2 (4)
AT→TA	7 (5)	1 (2)	8 (5)	3 (4)	1 (2)
Total	126	46	172	84	45
Tandem substitutions (tandem taken as one event)					
CC→TT	6 (50)	2 (50)	8 (50)	9 (90.0)	16 (100.0)
CC→AT	1 (8)	1 (25)	2 (13)	1 (10.0)	
CC→TG	1 (8)	1 (25)	2 (13)		
CT→TA	3 (25)		3 (19)		
TA→CT	1 (8)		1 (6)		
Total (% of tandem mutations)	12 (11)	4 (10)	16 (10)	10 (14)	16 (55)
Substitution location (tandem taken as one event)					
Py–Py site	111 (97)	36 (93)	150 (96)	65 (88)	45 (100)
Non-Py–Py site	3 (3)	3 (7)	6 (4)	9 (12)	0 (0)
Py–Py site location				Non-XP	XP-C + XP-A
Transcribed strand	8 (7)	2 (6)	10 (7)	30 (46)	0 (0)
Non-transcribed strand	103 (93)	34 (94)	140 (93)	35 (54)	11 (100)

[a]Data taken from van Kranen *et al.* (16) are included in the SKH-HRA column.[b]Data for human non-melanoma skin tumors are taken from several studies [see Reference (2) for review].

the high level of tandem mutations observed was not due to some specificity of the p53 biology but only to the typical signature of UV-induced lesions. If the four sites where both tandem and identical unique mutations on the same codon are pooled, resulting in the same amino acid changes (codons 123–124, 257–258, 263–264 and 271–272), then the frequency of tandem mutations is 28% on average, while the frequency of unique mutations is 72%. At CC sites, the probability of inducing tandem mutations is therefore quite high.

The data we have obtained from this large study clearly substantiates a major role for UV-B-induced photoproducts at dipyrimidine sites in murine *p53* mutagenesis and skin carcinogenesis. Furthermore, these results directly incriminate the loss of the p53 tumor suppressor function in the pathogenesis of UV-induced skin carcinomas in mice, and this can be used as an analogy to skin carcinomas in man (2,3). Recent results in humans and mice even indicate that the alteration of the *p53* gene by UV is probably an early event in the skin carcinogenesis process (11,28,29).

The positive predictive value of IHC for mutations in the conserved domains of the *p53* gene is 46% in this study, confirming the view put forward by Greenblatt *et al.* (5) that the status of the p53 protein by IHC cannot be equated with the wild-type or mutant genotype. This point has been fully discussed by Greenblatt *et al.* (5), including the hypothesis that mutations that occur in genes downstream of *p53* which can control p53 activity by feedback mechanisms. It is important to note, that we could discriminate quite clearly, based on the intensity of the CM-5 antibody staining, between a physiological response to DNA damage and a tumor related staining, because p53 staining seen as a response to DNA damage is less intense (29). Moreover, UV irradiation of the mice was stopped 72 h before the tumors were collected to avoid any discrepancy that might arise from any physiological response.

As in the three previous reports on UV-B-induced murine skin tumors (14–16) we have observed that most of the mutations of the *p53* gene (91%) are due to photolesions located on the non-transcribed strand of this gene. This strong strand bias is a reflection of the DNA repair mechanisms in rodent cells. Recent results have shown that cyclobutane pyrimidine dimers, which are one of the most prominent UV-induced DNA lesions, are preferentially removed from the transcribed strand and are hardly, or only very slowly, eliminated from the non-transcribed strand of the HPRT and the *p53* genes in rodent cells, as had been already observed in the XP group C cells (30,31).

Comparison of the murine and human p53 mutation spectra

The vast amount of data from human and mouse models have proven the suitability of the *p53* gene as a probe for studying mutagenesis. Good examples of a direct association between a specific carcinogen and a particular cancer has been seen by studying the human *p53* gene alteration patterns in lung cancers associated with benzo[*a*]pyrene found in cigarette smoke (32), in liver cancers associated with aflatoxin B1 consumption (33) and in skin cancers associated with solar exposure (2,3).

An important feature of the p53 protein is that it is highly conserved among vertebrates and therefore allows the extrapolation of carcinogenesis studies in animals to humans. For this reason, to assess the relevance of the hairless mouse model to human skin carcinogenesis, and hence evaluate the role of UV-B radiation in human skin carcinoma induction, we have compared the results obtained in two separate UV-B-induced murine skin cancer studies with those observed in

sun induced human skin cancers (Table II and Figure 2). Although *p53* mutation spectra in mice and human skin cancers were both UV-specific, they are not completely identical. GC to AT transitions are less frequent in skin tumors from normal individuals than in murine skin tumors, and substitutions are slightly more frequently found at dipyrimidine sites in murine and XP skin cancers than in normal human skin tumors. It is not clear whether these differences reflect differences in the DNA repair process between rodent and normal human cells or reflect the role of factors other than UV-B, for example UV-A in human skin carcinogenesis. As previously described, it has been demonstrated in mice that, dipyrimidine photolesions are preferentially removed from the transcribed strand and barely from the non-transcribed strand of active genes (30,31). This preferential repair of pyrimidine dimers also exists in human cells (34,35) but repair on the non-transcribed strand is faster than in murine cells. This variation in the repair process explains the differences observed in the strand bias for *p53* mutations between murine and non-XP human skin cancers, and could explain the divergence between these two *p53* mutation spectra. In fact, cells from the highly deficient repair group, XP-C, like rodent cells, repair only the transcribed strand of active genes, and indeed we found that all mutations of the *p53* gene in skin tumors from these patients were due to unrepaired UV-photolesions on the non-transcribed strand (10). This similarity in the DNA repair process between XP-C and mouse cells is therefore reflected by the same strand bias for *p53* mutations, but also very strikingly, by an almost identical mutation pattern when the type of base substitution and its location is considered (Table II).

Another hypothesis for explaining the differences between murine and human *p53* mutation spectra takes into consideration the role of factors other than UV-B, for example UV-A in the pathogenesis of skin cancers. UV-A radiation (>320 mm), which constitutes >90% of the solar energy, probably acts indirectly on DNA through interactions with cellular chromophores that subsequently generate reactive oxygen species (ROS) (27). These ROS usually attack G or A bases, and one of the base alterations produced by singlet oxygen is hydroxyguanine, which by mispairing with an A induces G→T transversions (36). This type of substitution represents 14% of the *p53* mutations in solar-induced human skin cancers but is rarely observed in UV-B-induced murine tumors (χ^2 test; $P < 0.02$). This significant difference could reflect the role of UV-A in human skin carcinogenesis. Only a few UV-A-induced mutation spectra have been reported in rodent or human cells (26,37) where mutations other than C→T have been found, and these were not located at dipyrimidine sequences.

Figure 2 allows a comparison of the distribution of *p53* mutations in exons 5 to 8 of the *p53* gene in skin tumors from humans and mice. Our analysis of a large number of samples has enabled us to define, for the first time, the existence of four distinct UV-mutation hot spots in the mouse *p53* mutation spectrum: two major ones at codons 267 (33%) and 272 (19%) and two minor ones at codons 146 (10%) and 173 (4%). It has already been shown that *p53* mutations in human skin carcinomas depend on at least two factors: first, on whether the site is a hot spot for UV photoproducts and/or a slow site for DNA repair (as seen at human amino acid 177, 196 and 278); and second, on whether a mutation at a particular site can disrupt or alter biological functions of the p53 protein (as seen at human amino acids 248, 273 and 282) (38). The hot spots for UV photoproducts and their repair rates have not been defined in the murine *p53* gene as yet, but their importance is clear: one of the two major UV-B murine hot spots that have been found at codon 272 corresponds to the human codon 278 skin cancer hot spot, which is known to be slowly repaired (38). This codon is not a mutation hot spot in internal tumors and thus confirms the importance of UV induced photolesions at this site in both the murine and human *p53* gene. Significantly, the other murine codon 267 mutation hot spot is an important UV-B mutable site, as it is a CpG preceded by a pyrimidine, whereas the equivalent human codon 273 is not a pronounced hot spot in human skin cancers as it lacks this dipyrimidine site. It should be noted that these mutations at codon 267 have only been found in studies of UV-B induced murine skin cancers (14–16) and not in other types of mouse tumors induced by a variety of carcinogens. In fact, in a mutation data base consisting of over 200 murine *p53* mutations, we have established that only one mutation is found at codon 267 and that the base that is changed is not the one involved in the majority of our UV-B induced codon 267 mutations. Hence, we can assume that UV-B is directly responsible for the mutations found at codon 267 in these tumors and that this mutation is strongly selected in the UV-B-induced murine skin carcinogenesis process. This amino acid is the equivalent of the human 273 amino acid, which is essential for the specific DNA binding activity of the human p53 protein, like the human amino acid 248, which is a mutation hot spot in human skin cancers. The variation in DNA-repair processes and slight interspecies variations in the DNA sequence of *p53* could then explain the disparity in mutation distribution between human and murine tumors.

The overall data presented here on UV-B-induced murine skin tumors confirms the role of UV-induced damage in the *p53* tumor suppressor gene inactivation during the skin carcinogenesis process. They also support the usefulness of the hairless mouse as it is only possible in animal models to evaluate the specificity of the UV wavelengths implicated in skin tumor induction and progression. Moreover, transgenic mice carrying mutated repair genes provide unique tools for analyzing the role of repair systems in counteracting the deleterious effects of UV irradiation. Finally, comparison of mouse *p53* mutation spectra with those obtained from humans strengthens the role of (solar) UV-B in human skin carcinoma induction by solar irradiation, and also indicates the possible involvement of other factors such as UV-A.

Acknowledgements

This work has been granted by the commission of the European Communities (contract no. EV5V-CT910030, Brussels, Belgium) and the Fondation de France (Paris, France). N.D. holds a fellowship from the Association pour la Recherche sur le Cancer (Villejuif, France).

References

1. International Agency for Research on Cancer (1993) *Health, Solar UV-radiation and Environmental Change*. IARC Technical report no. 13, Lyons, France.
2. Daya-Grosjean,L, Dumaz,N. and Sarasin,A. (1995) The specificity of *p53* mutation spectra in sunlight induced human cancers. *J. Photochem. Photobiol. B-Biol.*, **28**, 115–124.
3. Nataraj,A.J., Trent,J.C. and Ananthaswamy,H.N. (1995) *p53* Gene mutations and photocarcinogenesis. *Photochem. Photobiol.*, **62**, 218–230.
4. Ren,Z.P., Hedrum,A., Pontén,F., Nistér,M., Ahmadian,A., Lundeberg,J., Uhlén,M. and Pontén,J. (1996) Human epidermal cancer and accompanying precursors have identical *p53* mutations different from *p53* mutations in adjacent areas of clonally expanded non-neoplastic keratinocytes. *Oncogene*, **12**, 765–773.

5. Greenblatt,M.S., Bennett,W.P., Hollstein,M. and Harris,C.C. (1994) Mutations in the *p53* tumor suppressor gene: Clues to cancer etiology and molecular pathogenesis. *Cancer Res.*, **54**, 4855–4878.
6. Hollstein,M., Shomer,B., Greenblatt,M., Soussi,T., Hovig,E., Montesano,R. and Harris,C.C. (1996) Somatic point mutation in the *p53* gene of human tumors and cell lines: updated compilation. *Nucl. Acids Res.*, **24**, 141–146.
7. Brash,D.E., Rudolph,J.A., Simon,J.A., Lin,A., McKenna,G.J., Baden,H.P., Halparin,A.J. and Pontén,J. (1991) A role for sunlight in skin cancer: UV-induced *p53* mutations in squamous cell carcinoma. *Proc. Natl Acad. Sci. USA*, **88**, 10124–10128.
8. Ziegler,A., Leffell,D.J., Kunala,S. *et al*. (1993) Mutation hotspots due to sunlight in the *p53* gene of nonmelanoma skin cancers. *Proc. Natl Acad. Sci. USA*, **90**, 4216–4220.
9. Sato,M., Nishigori,C., Zghal,M., Yagi,T. and Takebe,H. (1993) Ultraviolet-specific mutations in *p53* gene in skin tumors in xeroderma pigmentosum patients. *Cancer Res.*, **53**, 2944–2946.
10. Dumaz,N., Drougard,C., Sarasin,A. and Daya-grosjean,L. (1993) Specific UV-induced mutation spectrum in the *p53* gene of skin tumors from DNA-repair-deficient xeroderma pigmentosum patients. *Proc. Natl Acad. Sci. USA*, **90**, 10529–10533.
11. Ziegler,A., Jonason,A.S., Leffell,D.J., Simon,J.A., Sharma,H.W., Kimmelman,J., Remington,L., Jacks,T. and Brash,D.E. (1994) Sunburn and *p53* in the onset of skin cancer. *Nature*, **372**, 773–776.
12. de Gruijl,F.R. and Forbes,P.D. (1995) UV-induced skin cancer in a hairless mouse model. *Bioessays*, **17**, 651–660.
13. de Gruijl,F.R., Sterenborg,H.J.C.M., Forbes,P.D. *et al*. (1993) Wavelength dependence of skin cancer induction by ultraviolet irradiation of albino hairless mice. *Cancer Res.*, **53**, 53–60.
14. Kress,S., Sutter,C., Strickland,P.T., Mukhtar,H., Schweizer,J. and Schwarz,M. (1992) Carcinogen-specific mutational pattern in the *p53* gene in ultraviolet-B radiation-induced squamous cell carcinomas of mouse skin. *Cancer Res.*, **52**, 6400–6403.
15. Kanjilal,S., Pierceall,W.E., Cummings,K.K., Kripke,M.L. and Ananthaswamy,H.N. (1993) High frequency of *p53* mutations in ultraviolet radiation-induced murine skin tumors – evidence for strand bias and tumor heterogeneity. *Cancer Res.*, **53**, 2961–2964.
16. van Kranen,H.J., de Gruijl,F.R., de Vries,A., Sontag,Y., Wester,P.W., Senden,H.C.M., Rozemuller,E. and van Kreijl,C.F. (1995) Frequent *p53* alterations but low incidence of *ras* mutations in UV-B-induced skin tumors of hairless mice. *Carcinogenesis*, **16**, 1141–1147.
17. de Gruijl,F.R. and van der Leun,J.C. (1991) Development of skin tumors in hairless mice after discontinuation of ultraviolet irradiation. *Cancer Res.*, **51**, 979–984.
18. Daya-Grosjean,L., Robert,C., Drougard,C., Suarez,H. and Sarasin,A. (1993) High mutation frequency in *ras* genes of skin tumors isolated from DNA repair deficient xeroderma-pigmentosum patients. *Cancer Res.*, **53**, 1625–1629.
19. Sambrook,J., Fritsch,E.F. and Maniatis,T. (1989) *Molecular Cloning*: *A Laboratory Manual*. Cold Spring Harbor Laboratory Press, Cold Spring Harbor, NY.
20. Condie,A., Eeles,R., Borresen,A.L., Coles,C., Cooper,C. and Prosser,J. (1993) Detection of point mutations in the *p53* gene — comparison of single-strand conformation polymorphism, constant denaturant gel electrophoresis, and hydroxylamine and osmium tetroxide techniques. *Hum. Mutat.*, **2**, 58–66.
21. Moyret,C., Theillet,C., Puig,P.L., Moles,J.P., Thomas,G., and Hamelin,R. (1994) Relative efficiency of denaturing gradient gel electrophoresis and single strand conformation polymorphism in the detection of mutations in exons 5 to 8 of the *p53* gene. *Oncogene*, **9**, 1739–1743.
22. Sheffield,V.C., Beck,J.S., Kwitek,A.E., Sandstrom,D.W. and Stone,E.M. (1993) The sensitivity of single-strand conformation polymorphism analysis for the detection of single base substitutions. *Genomics*, **16**, 325–332.
23. Vidal-Puig,A. and Moller,D.E. (1994) Comparative sensitivity of alternative single-strand conformation polymorphism (SSCP) methods. *Biotechniques*, **17**, 490–492, 494, 496.
24. Soussi,T., Caron de Fromentel,C. and May,P. (1990) Structural aspect of the p53 protein in relation to gene evolution. *Oncogene*, **5**, 945–952.
25. Armstrong,J.D. and Kunz,B.A. (1990) Site and strand specificity of UV-B mutagenesis in the SUP4-o gene of yeast [published erratum appears in *Proc. Natl Acad. Sci. USA*, **88**, 2035, 1991]. *Proc. Natl Acad. Sci. USA*, **87**, 9005–9009.
26. Drobetsky,E.A., Turcotte,J. and Chateauneuf,A. (1995) A role for ultraviolet A in solar mutagenesis. *Proc. Natl Acad. Sci. USA*, **92**, 2350–2354.
27. Hutchinson,F. (1994) Induction of tandem-base change mutations. *Mutat. Res.*, **309**, 11–15.
28. Nakazawa,H., English,D., Randell,P.L., Nakazawa,K., Martel,N., Armstrong,B.K. and Yamasaki,H. (1994) UV and skin cancer – specific *p53* gene mutation in normal skin as a biologically relevant exposure measurement. *Proc. Natl Acad. Sci. USA*, **91**, 360–364.
29. Berg,R.J.W., van Kranen,H.J., Rebel,H.G., de Vries,A., van Vloten,W.A., van Kreijl,C.F., van der Leun,J.C. and de Gruijl,F.R. (1996) Early *p53* alterations in mouse skin carcinogenesis by UV-B radiation: Immunohistochemical detection of mutant p53 protein in clusters of preneoplastic epidermal cells. *Proc. Natl Acad. Sci. USA*, **93**, 274–278.
30. Ruven,H.J.T., Berg,R.J.W., Seelen, C.M.J., Dekkers,J.A.J.M., Lohman,P.H.M., Mullenders,L.H.F. and van Zeeland,A.A. (1993) Ultraviolet-induced cyclobutane pyrimidine dimers are selectively removed from transcriptionally active genes in the epidermis of the hairless mouse. *Cancer Res.*, **53**, 1642–1645.
31. Ruven,H.J.T., Seelen,C.M.J., Lohman,P.H.M., van Kranen,H., van Zeeland,A.A. and Mullenders,L.H.F. (1994) Strand-specific removal of cyclobutane pyrimidine dimers from the *p53* gene in the epidermis of UV-B-irradiated hairless mice. *Oncogene*, **9**, 3427–3432.
32. Suzuki,H., Takahashi,T., Kuroishi,T., Suyama,M., Ariyoshi,Y. and Ueda,R. (1992) *p53* Mutations in non-small cell lung cancer in Japan: association between mutations and smoking. *Cancer Res.*, **52**, 734–736.
33. Aguilar,F., Hussain,S.P. and Cerutti,P. (1993) Aflatoxin-B(1) Induces the transversion of G→T in codon 249 of the *p53* tumor suppressor gene in human hepatocytes. *Proc. Natl Acad. Sci. USA*, **90**, 8586–8590.
34. Evans,M.K., Taffe,B.G., Harris,C.C. and Bohr,V.A. (1993) DNA strand bias in the repair of the *p53* gene in normal human and xeroderma-pigmentosum group-C fibroblasts. *Cancer Res.*, **53**, 5377–5381.
35. Ford,J.M., Lommel,L. and Hanawalt,P.C. (1994) Preferential repair of ultraviolet light-induced DNA damage in the transcribed strand of the human *p53* gene. *Mol. Carcinogen.*, **10**, 105–109.
36. Le Page,F., Margot,A., Grollman,A.P., Sarasin,A. and Gentil,A. (1995) Mutagenicity of a unique 8-oxoguanine in a human Ha-*ras* sequence in mammalian cells. *Carcinogenesis*, **16**, 2779–2784.
37. Robert,C., Muel,B., Benoit,A., Dubertret,L., Sarasin,A. and Stary,A. (1996) Cell survival and shuttle vector mutagenesis induced by ultraviolet A and ultraviolet B radiation in a human cell line. *J. Invest. Dermatol.*, **106**, 721–728.
38. Tornaletti,S. and Pfeifer,G.P. (1994) Slow repair of pyrimidine dimers at *p53* mutation hotspots in skin cancer. *Science*, **263**, 1436–1438.

Received on November 11, 1996; revised on January 16, 1997; accepted on January 21, 1997